

Indications of incommensurate spin fluctuations in doped triangular antiferromagnets

Ying Liang

Department of Physics, Beijing Normal University, Beijing 100875, China

Shiping Feng

Department of Physics and Key Laboratory of Beam Technology and Material Modification, Beijing Normal University, Beijing 100875, China

National Laboratory of Superconductivity, Academia Sinica, Beijing 100080, China

The incommensurate spin fluctuation of the doped triangular antiferromagnet is studied within the t - J model. It is shown that the commensurate peak near the half-filling is split into six incommensurate peaks in the underdoped and optimally doped regimes. The incommensurability increases with the hole concentration at lower dopings, and saturates at higher dopings. Although the incommensurability is almost energy independent, the weight of these incommensurate peaks decreases with energy and temperature.

74.25.Ha, 75.50.-y, 74.72.-h

The high- T_c cuprate superconductors exhibit many unusual properties^{1,2}, one of the most striking being the anomalous incommensurate antiferromagnetism in the normal state in the underdoped regime^{3,4}. These unusual properties are closely related to the fact that cuprate superconductors are doped Mott insulators, obtained by chemically adding charge carriers to a strongly correlated antiferromagnetic (AF) insulating state^{1,2}. Neutron-scattering measurements show that when the commensurate AF long-range-order (AFLRO) phase is suppressed and the hole concentration exceeds 3%, incommensurate dynamical short-range magnetic correlations appear^{3,4}, with four peaks located at the reciprocal space positions $[(1 \pm \delta)\pi, \pi]$ and $[\pi, (1 \pm \delta)\pi]$ (square lattice notations, unit lattice constant). Even more remarkable is that for very low dopings the incommensurability δ varies almost linearly with the concentration x , but saturates at higher dopings. Moreover, the incommensurate peaks broaden and weaken in amplitude as the energy increases. This incommensurate antiferromagnetism of doped cuprates results from special microscopic conditions^{3,4}: (1) Cu ions situated in a square-planar arrangement and bridged by oxygen ions, (2) weak coupling between neighboring layers, and (3) doping in such a way that the Fermi level lies near the middle of the Cu-O σ^* bond. One common feature of these doped cuprates is the *square-planar* Cu arrangement. However, some materials with a two-dimensional (2D) spin arrangements on non-square lattices have been synthesized. In particular, it has been reported⁵ that there is a class of doped cuprates, $\text{RCuO}_{2+\delta}$, R being a rare-earth element, where the Cu ions sites sit not on a square-planar, but on a *triangular-planar lattice*, therefore allowing a test of the geometry effect on the spin fluctuations, while retaining some other unique microscopic features of the Cu-O bond. In other words, the question is whether the incommensurate magnetic fluctuations observed on the doped square antiferromagnet exist also in the doped triangular antiferromagnet? In addition, the doped triangular antiferromagnet, where geometric frustration is present, is also of theo-

retical interest by himself, with many unanswered fascinating theoretical questions⁶. Historically the undoped triangular antiferromagnet was firstly proposed to be a model for microscopic realization of the resonating valence bond spin liquid due to the strong frustration⁷. It has been argued⁸ that this spin liquid state plays a crucial role in the superconductivity of doped cuprates. Moreover, it has been shown⁹ that the doped and undoped triangular antiferromagnets present a pairing instability in an unconventional channel.

The incommensurate antiferromagnetism of the doped square antiferromagnet has been extensively studied, and some fundamentally different microscopic mechanisms have been proposed¹⁰⁻¹² to explain the origin of the incommensurate antiferromagnetism, where there is a general consensus that incommensurate antiferromagnetism emerges due to doped charge carriers. Recently, it has been shown very clearly¹³ that if the strong electron correlation is treated properly and strong spinon-holon interaction is taken into account, the t - J model can correctly reproduce all main features of the incommensurate antiferromagnetism in the underdoped square antiferromagnets, including the doping dependence of the incommensurate peak position and the energy dependence of the amplitude of these peaks. Since the strong electron correlations are present in both doped square and triangular antiferromagnets, it is expected that the unconventional incommensurate antiferromagnetism existing in the doped square antiferromagnet may also be seen in the doped triangular antiferromagnet. In this paper, the purpose is to apply the successful approach¹³ for the doped square lattice antiferromagnet to triangular lattice. We hope that the information from the present work may induce further experimental works in doped antiferromagnets on the non-square lattice.

As in the doped square antiferromagnet, the essential physics of the doped triangular antiferromagnet is well described by the t - J model on the triangular lattice,

$$\begin{aligned}
H = & -t \sum_{i\hat{\eta}\sigma} C_{i\sigma}^\dagger C_{i+\hat{\eta}\sigma} + \text{h.c.} - \mu \sum_{i\sigma} C_{i\sigma}^\dagger C_{i\sigma} \\
& + J \sum_{i\hat{\eta}} \mathbf{S}_i \cdot \mathbf{S}_{i+\hat{\eta}}, \quad (1)
\end{aligned}$$

with the electron single occupancy local constraint $\sum_{\sigma} C_{i\sigma}^\dagger C_{i\sigma} \leq 1$, where the summation is over all sites i , and for each i , over its nearest-neighbor $\hat{\eta}$, $\mathbf{S}_i = C_{i\sigma}^\dagger \vec{\sigma} C_{i\sigma} / 2$ are spin operators with $\vec{\sigma} = (\sigma_x, \sigma_y, \sigma_z)$ as Pauli matrices, and μ is the chemical potential. In the t - J model (1), the strong electron correlation manifests itself by the local constraint⁸, therefore the crucial requirement is to impose this local constraint. It has been shown¹⁴ that this constraint can be treated properly in analytical calculations within the fermion-spin theory based on the charge-spin separation, where the constrained electron operators are decomposed $C_{i\uparrow} = h_i^\dagger S_i^-$ and $C_{i\downarrow} = h_i^\dagger S_i^+$, where the spinless fermion operator h_i describes the charge (holon) degrees of freedom, while the pseudospin operator S_i describes the spin (spinon) degrees of freedom, then the low energy behavior of the t - J model (1) on the triangular lattice in the fermion-spin representation can be written as¹⁴,

$$\begin{aligned}
H = & -t \sum_{i\hat{\eta}} h_i h_{i+\hat{\eta}}^\dagger (S_i^+ S_{i+\hat{\eta}}^- + S_i^- S_{i+\hat{\eta}}^+) + \mu \sum_i h_i^\dagger h_i \\
& + J_{\text{eff}} \sum_{i\hat{\eta}} \mathbf{S}_i \cdot \mathbf{S}_{i+\hat{\eta}}, \quad (2)
\end{aligned}$$

where $J_{\text{eff}} = [(1-\delta)^2 - \phi^2]$, δ is the hole doping concentration, and $\phi = \langle h_i^\dagger h_{i+\hat{\eta}} \rangle$ is the holon particle-hole order parameter. At half-filling, the t - J model is simply the Heisenberg model. Many authors have shown that as in the square lattice, there is indeed AFLRO in the ground state of the AF triangular Heisenberg model¹⁵, but this AFLRO is destroyed more rapidly with increasing dopings than on the square lattice due to the strong geometric frustration, then away from the half-filling, there

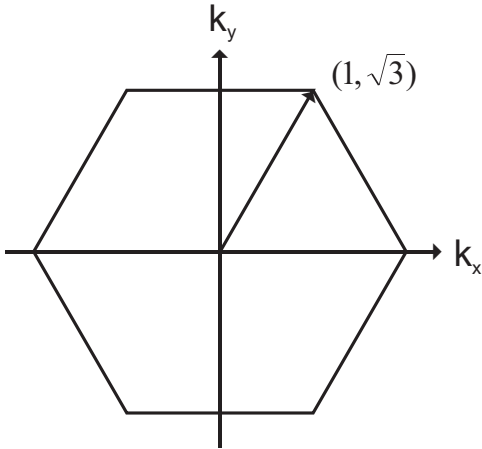


FIG. 1. The Brillouin zone for the triangular system, where the antiferromagnetic wave vector $Q = [1, \sqrt{3}]$.

is no AFLRO for the doped triangular antiferromagnet, *i.e.*, $\langle S_i^z \rangle = 0$, and holons move self-consistently in the background of the spinon liquid state.

Within the framework of the fermion-spin theory, the spin fluctuations couple only to spinons, but the strong correlation between holons and spinon is included through the holon's order parameter ϕ entering the spinon propagator, therefore both spinons and holons are responsible for the spin fluctuation. In this case, the incommensurate spin dynamics in the doped square antiferromagnet and integrated spin response in the doped triangular antiferromagnet have been discussed^{13,16} by considering the spin fluctuation around the mean-field (MF) solution, where the spinon part is treated by a loop expansion to second-order. Following their discussions^{13,16}, we can obtain the dynamical spin structure factor for the doped triangular antiferromagnet as,

$$\begin{aligned}
S(\mathbf{k}, \omega) = & -2[1 + n_B(\omega)] \text{Im}D(\mathbf{k}, \omega) = -2[1 + n_B(\omega)] \\
& \times \frac{B_k^2 \text{Im}\Sigma_s(\mathbf{k}, \omega)}{[\omega^2 - \omega_k^2 - B_k \text{Re}\Sigma_s(\mathbf{k}, \omega)]^2 + [B_k \text{Im}\Sigma_s(\mathbf{k}, \omega)]^2}, \quad (3)
\end{aligned}$$

where the full spinon Green's function, $D^{-1}(\mathbf{k}, \omega) = D^{(0)-1}(\mathbf{k}, \omega) - \Sigma_s(\mathbf{k}, \omega)$, and the MF spinon Green's function $D^{(0)-1}(\mathbf{k}, \omega) = (\omega^2 - \omega_k^2) / B_k$, $\text{Im}\Sigma_s(\mathbf{k}, \omega)$ and $\text{Re}\Sigma_s(\mathbf{k}, \omega)$ being the imaginary and real parts of the second order spinon self-energy, respectively. They are obtained from the holon bubble,

$$\Sigma_s(\mathbf{k}, \omega) = - \left(\frac{Zt}{N} \right)^2 \sum_{pp'} (\gamma_{k-p} + \gamma_{p'+p+k})^2 \frac{B_{k+p'}}{2\omega_{k+p'}}$$

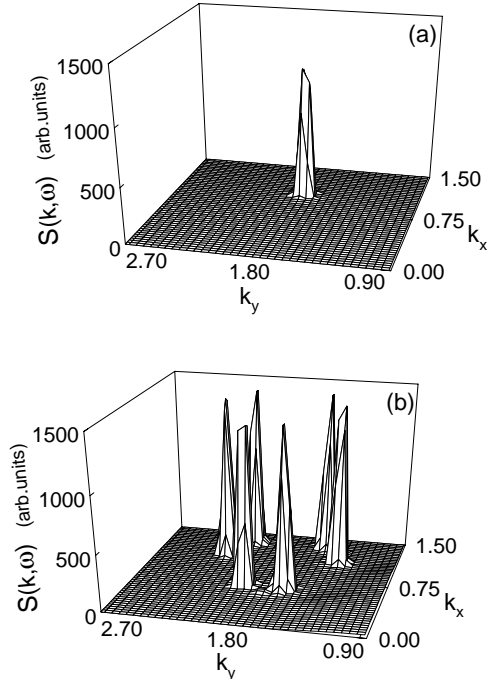


FIG. 2. The dynamical spin structure factor in the (k_x, k_y) plane at doping (a) $x = 0.015$ and (b) $x = 0.06$ at temperature $T = 0.15J$ and energy $\omega = 0.05J$ for parameter $t/J = 2.5$.

$$\times \left(\frac{F_1(k, p, p')}{\omega + \xi_{p+p'} - \xi_p + \omega_{k+p'}} - \frac{F_2(k, p, p')}{\omega + \xi_{p+p'} - \xi_p - \omega_{k+p'}} \right), \quad (4)$$

where $B_k = \Delta[(2\epsilon\chi_z + \chi)\gamma_k - (\epsilon\chi + 2\chi_z)]$, $\Delta = 2ZJ_{eff}$, $\epsilon = 1 + 2t\phi/J_{eff}$, $\gamma_k = [\cos k_x + 2\cos(k_x/2)\cos(\sqrt{3}k_y/2)]/3$, Z is the number of the nearest neighbor sites, $F_1(k, p, p') = n_F(\xi_{p+p'})[1 - n_F(\xi_p)] + [1 + n_B(\omega_{k+p'})][n_F(\xi_p) - n_F(\xi_{p+p'})]$, $F_2(k, p, p') = n_F(\xi_{p+p'})[1 - n_F(\xi_p)] - n_B(\omega_{k+p'})[n_F(\xi_p) - n_F(\xi_{p+p'})]$, $n_F(\xi_k)$ and $n_B(\omega_k)$ are the fermion and boson distribution function, respectively, the MF holon excitation $\xi_k = 2\chi t Z \gamma_k + \mu$, and MF spinon excitation, $\omega_k^2 = \Delta^2(A_1\gamma_k^2 + A_2\gamma_k + A_3)$ with $A_1 = \alpha\epsilon(\chi/2 + \epsilon\chi_z)$, $A_2 = \epsilon[(1 - Z)\alpha(\epsilon\chi/2 + \chi_z)/Z - \alpha(C_z + C/2) - (1 - \alpha)/(2Z)]$, $A_3 = \alpha(C_z + \epsilon^2 C/2) + (1 - \alpha)(1 + \epsilon^2)/(4Z) - \alpha\epsilon(\chi/2 + \epsilon\chi_z)/Z$, the spinon correlation functions $\chi = \langle S_i^+ S_{i+\hat{\eta}}^- \rangle$, $\chi_z = \langle S_i^z S_{i+\hat{\eta}}^z \rangle$, $C = (1/Z^2) \sum_{\hat{\eta}\hat{\eta}'} \langle S_{i+\hat{\eta}}^+ S_{i+\hat{\eta}'}^- \rangle$, and $C_z = (1/Z^2) \sum_{\hat{\eta}\hat{\eta}'} \langle S_{i+\hat{\eta}}^z S_{i+\hat{\eta}'}^z \rangle$. In order to satisfy the sum rule for the correlation function $\langle S_i^+ S_i^- \rangle = 1/2$ in the absence of AFLRO, a decoupling parameter α has been introduced in the self-consistent MF calculation, which can be regarded as the vertex correction¹⁷.

The Brillouin zone of the triangular system is shown in Fig. 1, where the AF wave vector $\mathbf{Q} = [1, \sqrt{3}]$ (hereafter we use the units of $[2\pi/3, 2\pi/3]$). In Fig. 2, we plot the dynamical spin structure factor $S(\mathbf{k}, \omega)$ in the $[k_x, k_y]$ plane at doping (a) $x = 0.015$ and (b) $x = 0.06$ with temperature $T = 0.15J$ and energy $\omega = 0.05J$ for parameter $t/J = 2.5$. From Fig. 2, we find that a commensurate-incommensurate transition in the spin fluctuation \mathbf{Q} vector occurs with doping, *i.e.*, the commensurate peak near half-filling ($x \leq 0.015$) is split into six peaks in the underdoped regime, while the positions of these split peaks are incommensurate with the underlying lattice, and correspond to six 2D rods at $[(1 - \delta_x), (\sqrt{3} \pm \delta_y)]$, $[(1 - \delta'_x), (\sqrt{3} \pm \delta'_y)]$, and $[(1 - \delta''_x), (\sqrt{3} \pm \delta''_y)]$ with

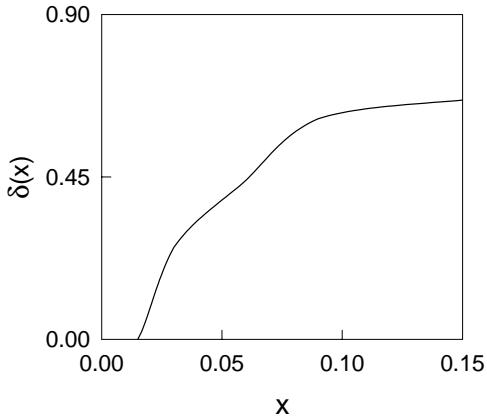


FIG. 3. The doping dependence of the incommensurability $\delta(x)$ of the antiferromagnetic fluctuations.

$\sqrt{\delta_x^2 + \delta_y^2} = \sqrt{(\delta'_x)^2 + (\delta'_y)^2} = \sqrt{(\delta''_x)^2 + (\delta''_y)^2} = \delta$. At low temperatures, the incommensurate peaks are very sharp at lower energies, which means that these excitations have a dynamical coherence length that is larger than the instantaneous correlation length. The present dynamical spin structure factor spectrum $S(\mathbf{k}, \omega)$ has been used to extract the doping dependence of the incommensurability parameter $\delta(x)$, defined as the deviation of the peak position from the AF wave vector \mathbf{Q} , and the result is plotted in Fig. 3. Our result shows that $\delta(x)$ increases with the hole concentration in lower dopings, but it saturates at higher dopings, which is qualitatively similar to the results for the square antiferromagnet^{3,4,13}.

In order to study the effects of energy and temperature on the incommensurate spin fluctuation, we have calculated the dynamical spin structure factor $S(\mathbf{k}, \omega)$ at different temperatures and energies, and the result at doping $x = 0.06$ for parameter $t/J = 2.5$, temperature $T = 0.15J$ and energy $\omega = 0.1J$ is shown in Fig. 4. In comparison with Fig. 2(b) for the same set of parameters except for $\omega = 0.05J$, we see that although the positions of the incommensurate peaks are almost energy independent, the weight of these peaks decreases with increasing energy, and tends to vanish at high energies. This reflects that the inverse lifetime of the spin

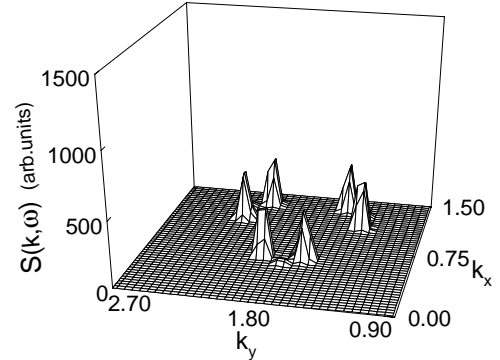


FIG. 4. The dynamical spin structure factor in the (k_x, k_y) plane at doping $x = 0.06$ for parameter $t/J = 2.5$ and energy $\omega = 0.1J$ at temperature $T = 0.15J$.

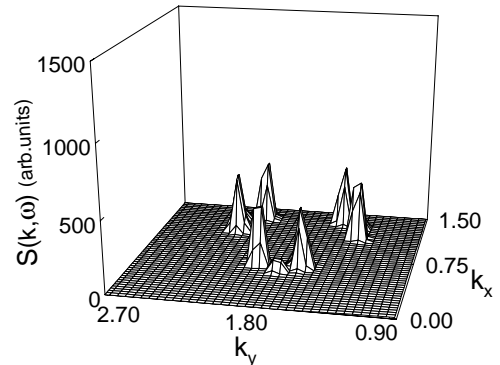


FIG. 5. The dynamical spin structure factor in the (k_x, k_y) plane at doping $x = 0.06$ for parameter $t/J = 2.5$ and energy $\omega = 0.05J$ at temperature $T = 0.3J$.

excitations increases with increasing energy. In correspondence, the dynamical spin structure factor $S(\mathbf{k}, \omega)$ at doping $x = 0.06$ for parameter $t/J = 2.5$ in energy $\omega = 0.05J$ and temperature $T = 0.3J$ is plotted in Fig. 5. Comparing with Fig. 2(b) for the same set of parameters except for $T = 0.15J$, we find that the peak weight is suppressed with increasing temperature. Our results also indicate that although the positions of the incommensurate peaks in the doped triangular antiferromagnets are much different from these in the doped square antiferromagnets due to the geometric frustration, the behavior of the energy and temperature dependence of the magnetic fluctuation is qualitatively similar to these in the doped square antiferromagnets^{3,4,13}.

As in the case of the doped square antiferromagnet¹³, the effect of holons on the spinons due to the strong spinon-holon interaction is critical in determining the characteristic feature of the incommensurate spin fluctuation in the doped triangular antiferromagnet. This is reflected by the renormalization of the spinon excitation $E_k^2 = \omega_k^2 + B_k \text{Re}\Sigma_s(k, E_k)$ in Eq. (3). Figure 6 shows this renormalized spinon excitation for doping $x = 0.015$ (solid line), $x = 0.03$ (dashed line), and $x = 0.06$ (dot-dashed line), and for $t/J = 2.5$ and $T = 0.15J$. An over damping around the AF wave vector \mathbf{Q} occurs for doping $x \geq 0.015$. The incommensurate peaks emerge in the dy-

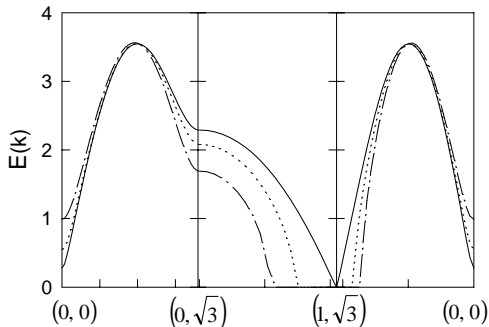


FIG. 6. The spinon excitation spectrum at doping $x = 0.015$ (solid line), $x = 0.03$ (dashed line), and $x = 0.06$ (dot-dashed line) in parameter $t/J = 2.5$ with temperature $T = 0.15J$.

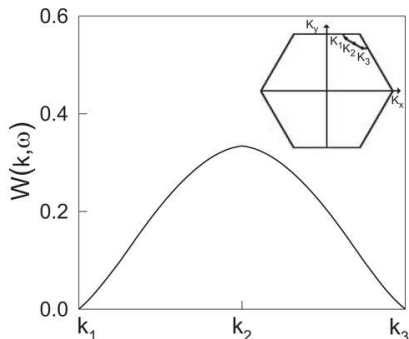


FIG. 7. Function $W(\mathbf{k}, \omega)$ at doping $x = 0.06$ for parameter $t/J = 2.5$ and energy $\omega = 0.05J$ at temperatures $T = 0.15J$.

namical spin structure factor $S(\mathbf{k}, \omega)$ when the incoming neutron energy ω is equal to the renormalized spin excitation E_k , *i.e.* $W(\mathbf{k}_\delta, \omega) \equiv [\omega^2 - \omega_{k_\delta}^2 - B_{k_\delta} \text{Re}\Sigma_s(\mathbf{k}_\delta, \omega)]^2 = (\omega^2 - E_{k_\delta}^2)^2 \sim 0$ for some critical wave vectors \mathbf{k}_δ (positions of the incommensurate peaks). Then the weight of these peaks is determined by the imaginary part of the spinon self-energy $1/\text{Im}\Sigma_s(\mathbf{k}_\delta, \omega)$. Therefore near half-filling, the spin excitations are centered around the AF wave vector \mathbf{Q} , so the commensurate AF peak appears there. Upon doping, the holes disturb the AF background self-consistently, and induce over damping of the spinon excitation around the AF wave vector \mathbf{Q} , leading to incommensurate antiferromagnetism. Since the weight of the incommensurate peaks is determined by the imaginary part of the spinon self-energy, it is then understandable that they are suppressed as energy and temperature are increased. Moreover, the symmetry of the incommensurate pattern is determined by the lattice symmetry in the spinon self-energy renormalization due to holons. We have plotted the function $W(\mathbf{k}, \omega)$ along the line shown in the inset of Fig. 7 at doping $x = 0.06$ for parameter $t/J = 2.5$ and temperature $T = 0.15J$ and energy $\omega = 0.05J$ in Fig. 7. There is a strong angular dependence with minima at $[(1 - \delta_x), (\sqrt{3} - \delta_y)]$, $[(1 - \delta'_x), (\sqrt{3} - \delta'_y)]$. These are exactly the positions of the incommensurate peaks determined by the dispersion of very well defined renormalized spin excitations. This incommensurate pattern is much different from that in the doped square antiferromagnet¹³, since the lattice symmetry in the triangular lattice is much different from that in the square lattice.

In summary, we have discussed the incommensurate spin fluctuation of the doped triangular antiferromagnet within the t - J model based on the fermion-spin theory. It is shown that the commensurate peak near the half-filling is split into six incommensurate peaks in the underdoped and optimally doped regimes. The incommensurability increases with the hole concentration at lower dopings, and saturates at higher dopings. Although the incommensurability is almost energy independent, the weight of these incommensurate peaks decreases with energy and temperature.

ACKNOWLEDGMENTS

The authors would like to thank Dr. Feng Yuan for helpful discussions. This work was supported by the National Natural Science Foundation under the Grant No. 10074007, 10125415, and 90103024, and the Grant from Ministry of Education of China.

- ¹ See, e.g., *Proceedings of Los Alamos Symposium*, edited by K.S. Bedell, D. Coffey, D.E. Meltzer, D. Pines, and J.R. Schrieffer (Addison-Wesley, Redwood city, California, 1990).
- ² A. P. Kampf, Phys. Rep. **249**, 219 (1994); M. A. Kastner, R. J. Birgeneau, G. Shiran, Y. Endoh, Rev. Mod. Phys. **70**, 897 (1998).
- ³ K. Yamada, C.H. Lee, K. Kurahashi, J. Wada, S. Wakimoto, S. Ueki, H. Kimura, Y. Endoh, S. Hosoya, and G. Shirane, Phys. Rev. B **57**, 6165 (1998), and references therein.
- ⁴ P. Dai, H.A. Mook, R.D. Hunt, and F. Doğan, Phys. Rev. B **63**, 54525 (2001), and references therein.
- ⁵ A.P. Ramirez, R.J. Cava, J.J. Krajewski, and W.F. Peck, Jr., Phys. Rev. B **49**, 16082 (1994); R.J. Cava, H.W. Zandbergen, A.P. Ramirez, H. Takagi, C.T. Chen, J.J. Krajewski, W.F. Peck, Jr., J.V. Waszczak, G. Meigs, and L.F. Schneemeyer, J. Solid State Chem. **104**, 437 (1993).
- ⁶ S. Sachdev, Phys. Rev. B **45**, 12377 (1992).
- ⁷ P.W. Anderson, Mater. Res. Bull. **8**, 153 (1973); P. Fazekas and P.W. Anderson, Philos. Mag. **30**, 423 (1974).
- ⁸ P.W. Anderson, Science **235**, 1196 (1987); F.C. Zhang and T.M. Rice, Phys. Rev. B **37**, 3759 (1988).
- ⁹ R.B. Laughlin, Phys. Rev. Lett. **60**, 2677 (1988); M. Vojta and E. Dagotto, Phys. Rev. B **59**, R713 (1999).
- ¹⁰ A. Aharony, R.J. Birgeneau, A. Coniglio, M.A. Kastner, and H.E. Stanley, Phys. Rev. Lett. **60**, 1330 (1988); D. Poilblanc and T.M. Rice, Phys. Rev. B **39**, 9749 (1989); H.J. Schulz, Phys. Rev. Lett. **64**, 1445 (1990).
- ¹¹ N. Bulut, D. Hone, D.J. Scalapino, and N.E. Bickers, Phys. Rev. Lett. **64**, 2723 (1990); Q. Si, Y. Zha, K. Levin, and J.P. Lu, Phys. Rev. B **47**, 9055 (1993); P.B. Littlewood, J. Zaanen, G. Aeppli, and H. Monien, Phys. Rev. B **48**, 487 (1993); S. Sachdev, C. Buragohain, M. Vojta, Science **286**, 2479 (1999).
- ¹² E. Dagotto, Rev. Mod. Phys. **66**, 763 (1994), and references therein.
- ¹³ Feng Yuan, Shiping Feng, Zhao-Bin Su, and Lu Yu, Phys. Rev. B **64**, 224505 (2001).
- ¹⁴ Shiping Feng, Z.B. Su, and L. Yu, Phys. Rev. B **49**, 2368 (1994); Mod. Phys. Lett. B **7**, 1013 (1993).
- ¹⁵ L. Capriotti, A. E. Trumper, and S. Sorella, Phys. Rev. Lett. **82**, 3899 (1999).
- ¹⁶ Pengpeng Zhang, Shiping Feng, and Wei Yeu Chen, Phys. Rev. B **62**, 13828 (2000).
- ¹⁷ J. Kondo and K. Yamaji, Prog. Theor. Phys. **47**, 807 (1972); Shiping Feng and Yun Song, Phys. Rev. B **55**, 642 (1997).